Multiple steps and multiple excitations in photoisomerization of azobenzene

ARTICLE *in* CHEMICAL PHYSICS LETTERS · JANUARY 2008

Impact Factor: 1.9 · DOI: 10.1016/j.cplett.2007.11.009

2 AUTHORS, INCLUDING:

Roland E. Allen
Texas A&M University
242 PUBLICATIONS **3,459** CITATIONS

Available online at www.sciencedirect.com
ScienceDirect
Chemical Physics Letters 450 (2008) 192–195
CHEMICAL PHYSICS LETTERS
www.elsevier.com/locate/cplett

Multiple steps and multiple excitations in photoisomerization of azobenzene

Petra Sauer, Roland E. Allen *

Department of Physics, Texas A&M University, College Station, TX 77843, United States

Received 14 July 2007; in final form 2 November 2007
Available online 7 November 2007

Abstract

Detailed understanding of femtosecond-scale photochemical processes requires dynamical simulations that are complementary to interpretations based on transitions between energy surfaces. For *cis* to *trans* photoisomerization of azobenzene following a 100 fs laser pulse, we find that the mechanism is rotation about the central NN bond, and the process is complete in less than 1 ps. The initial excitation and subsequent de-excitation are each achieved via multiple steps, with the molecule always in a superposition of electronic states, as the 3N nuclear degrees of freedom are excited by the laser pulse.

Molecules that can be reversibly switched between distinct states, with different structural, physical, and electronic properties, are currently of considerable interest for various reasons, including their potential applications in molecular electronics [1,2]. Among these molecules are azobenzene and its derivatives, which undergo changes in conformation upon photoexcitation. In addition to having distinct structural forms that are separated by a relatively large energy barrier, the shorter *cis* isomer and the longer *trans* isomer (see Fig. 1) have very different calculated conductances [3]. Derivatives of azobenzene have been successfully demonstrated to have a wide variety of potentially important applications, including use in photoelectrochemical storage [4], liquid crystal display devices [5], nanomechanical devices [6], holographic storage [7], guiding mechanisms for the motion of liquid droplets [8], instigators of protein folding [9], and optical switches for protein activity [10].

Cis to *trans* isomerization can occur following a transition into either the first $(n \rightarrow \pi^*, S_1)$ or the second $(\pi \rightarrow \pi^*, S_2)$ excited state, although the photoisomerization quantum yield for S_1 is significantly larger than that for S_2 [11]. Absorption spectroscopy measurements for excitation to the first excited state have shown that the formation of the dominant photoproduct occurs within 170 fs [12]. The difference in quantum yields originally led to a suggestion that there are two mechanisms for isomerization: In this picture, molecules excited to the S_1 state isomerize by an inversion which involves in-plane bending of a CNN bond angle, whereas molecules excited to the S_2 state isomerize through a rotation around the NN bond. One of the earliest theoretical calculations, which used configuration interaction with a small basis set to determine the ground-state and excited-state energy surfaces, provided support for the picture that isomerization proceeds via the inversion mechanism in the first excited state [13]. On the other hand, some of the more recent calculations, using a complete active space self-consistent field approach (CASSCF) [14–16], density functional theory (DFT) [17], and a semiempirical method [18], have found a conical intersection between the ground-state S_0 and the first excited state S_1 near the midpoint of the rotational pathway, indicating that rotation about the central NN bond, rather than inversion through a CNN bond, is the preferred mechanism for isomerization.

Recent theoretical calculations have shown the existence of a third excited state S_3, consisting of a doubly excited

* Corresponding author. Fax: +1 979 845 2590.
E-mail address: allen@tamu.edu (R.E. Allen).

0009-2614/$ - see front matter © 2007 Elsevier B.V. All rights reserved.
doi:10.1016/j.cplett.2007.11.009

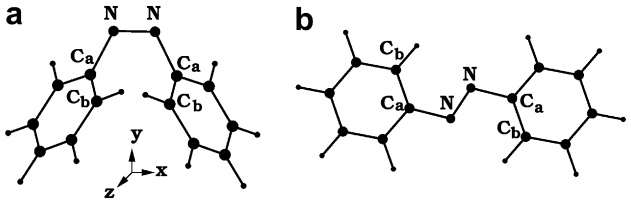

Fig. 1. Ground-state structures of (a) *cis* and (b) *trans* forms of azobenzene, as calculated with the present (SERID) method.

$n^2\pi^{*2}$ configuration that has a deep minimum approximately halfway between the *cis* and *trans* configurations along a torsional pathway [19,20]. The potential energy curve for this state crosses that of the S_2 state, offering an explanation for the short lifetime of S_2.

Here we examine in detail the *cis* to *trans* photoisomerization of azobenzene following a laser pulse with a duration of 100 fs (full width at half maximum, or FWHM) and an effective photon energy initially matched to the first excited state transition.

The calculations employ semiclassical electron-radiation-ion dynamics (SERID), a method which is described in detail elsewhere [21] and is particularly well suited to studies of the rich variety of ultrafast chemical phenomena reviewed by, e.g., Zewail [22]. The nuclear motion and radiation field are treated classically, while the dynamics of the valence electrons is treated via solution of the time-dependent Schrödinger equation at each time step, in a nonorthogonal basis. As discussed in detail in our previous paper [23], a semiclassical description omits only effects that are second-order in the quantum fluctuations of nuclei and radiation field, and effectively includes *n*-photon and *n*-phonon transitions (just as they are effectively included in time-dependent perturbation theory, and with 'phonon' meaning 'vibrational quantum'). The method also effectively includes doubly excited states like the $S_3(n^2\pi^{*2})$ state discussed above and in Refs. [19,20].

The Hamiltonian matrix, overlap matrix, and effective ion–ion repulsion were derived from density-functional calculations [24,25]. Although higher levels of theory have been shown to give a more accurate quantitative description of azobenzene [26], DFT calculations capture the key structural and electronic features of this molecule [17,27], while permitting large-scale computational studies like those described here. With the SERID method, we can monitor the interplay between nuclear motion and changes involving the electronic states. These dynamical processes result from both laser pulse excitation and population transfer via transitions at avoided crossings of the electronic energy levels.

The ground-state geometries of both the *cis* and the *trans* forms of azobenzene, show in Fig. 1, were obtained through 2000 fs simulations in which the velocity of each atom was reduced by 0.03% after each 10 as time step. The bond lengths, bond angles, and energies are in good agreement with accepted values [8,13–18,26,27]. The *trans* isomer, with C_{2h} symmetry, has a HOMO − 1 state which is characterized by NN π bonding, a HOMO characterized by nonbonding (*n*) atomic orbitals on these central nitrogen atoms, and a LUMO characterized by an NN π^* antibonding interaction. The *cis* isomer has C_2 symmetry; because of its non-planarity, the HOMO − 1 and HOMO states have a mixture of n and π character, and the LUMO again is characterized by a π^* antibonding interaction in the NN bond. The HOMO − 1 orbital for this *cis* isomer is nearly degenerate with two other occupied π orbitals, which lie slightly lower in energy in the present (density-functional-based) model.

A 100 fs laser pulse with a fluence of 0.473 kJ/m^2 and a polarization in the (1,1,1) direction (see Fig. 1) was then applied to the equilibrated *cis* isomer. This value of the fluence was chosen because we found in other simulations (not shown here) that substantially smaller fluences do not result in isomerization and substantially larger fluences lead to photodissociation. The effective photon energy of the pulse was matched to the HOMO–LUMO energy gap for the initial ground-state geometry of the molecule, which is 3.55 eV in the present density-functional-based model. As can be seen in Fig. 2, the initial excitation is from HOMO to LUMO, transferring roughly 0.2 electrons into the excited state.

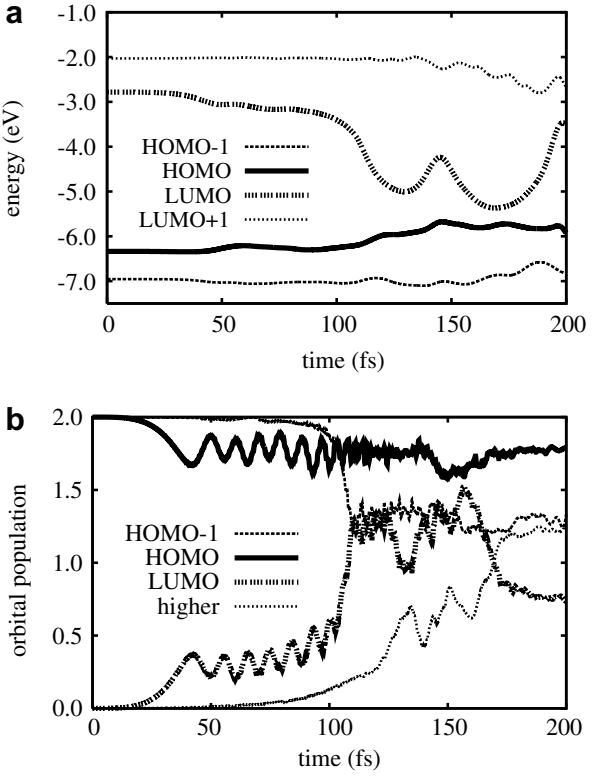

Fig. 2. (a) Energy levels and (b) populations of molecular orbitals in *cis*-azobenzene during application of 100 fs (FWHM) pulse with a fluence of 0.473 kJ/m^2 and an effective photon energy of 3.55 eV. In (b), the populations of all electronic states above the LUMO are combined in one curve. The full duration of the laser pulse spans the interval shown, from 0 to 200 fs.

This change in electronic population excites various vibrational modes in the molecule via Hellmann–Feynman forces. Initially the magnitude of the central C_aNNC_a dihedral angle (Fig. 3a) increases, while the C_bC_aNN dihedral angles (Fig. 3b) decrease in size. These geometrical changes lower the energy of the LUMO, so that the effective photon energy of the laser pulse is no longer resonant with the HOMO to LUMO energy gap, but instead becomes more nearly in resonance with the HOMO − 1 to LUMO energy difference (see Fig. 2a). At about 100 fs, a second excitation, from HOMO − 1 to LUMO, then transfers an additional 1.0 electrons into the LUMO (Fig. 2b). The forces due to this electronic population redistribution further stimulate the nuclear motion, so that at 150 fs the magnitude of the C_aNNC_a angle has increased to 55°, while the magnitudes of the two C_bC_aNN angles have decreased to approximately 15°. As can be seen in the time interval between 0 fs and 120 fs, these geometrical changes result in a substantial total decrease in the HOMO–LUMO energy gap.

In addition, the LUMO exhibits some oscillatory behavior, reaching a minimum at 127 fs and again at 170 fs. This behavior results from oscillations of the central NN bond, which (although not shown here) reaches maximum values at the same times that the LUMO energy reaches minima. The coupling between the time-dependent geometry and the time-dependent electronic energy levels is thus clearly apparent, even though both geometry and electronic structure involve many degrees of freedom.

As the LUMO energy further decreases, the HOMO − 1 to LUMO energy difference eventually falls out of resonance with the effective photon energy $\hbar\omega$ of the laser pulse, but the energy differences between the LUMO and several nearly degenerate higher-lying orbitals become nearly resonant with $\hbar\omega$. As a result, roughly 0.45 electrons are transferred from the LUMO to these higher-lying states. At the end of the laser pulse, approximately 0.75 electrons are in the LUMO, 0.2 holes in the HOMO, and 0.8 holes in the HOMO − 1. There are also additional holes in the lower-lying occupied states, and additional electrons in the higher-lying unoccupied states, but these do not play a significant role in the isomerization process described below.

After completion of the laser pulse, the first significant transfer of electronic population occurs roughly 260 fs into the simulation. At this time there is an avoided crossing between the HOMO − 1 and HOMO levels that transfers approximately 0.7 holes from the HOMO − 1 into the HOMO (see Fig. 4). During this initial population transfer, the C_aNNC_a and C_bC_aNN dihedral angles are respectively near 0° and 60° (Fig. 3). Immediately afterward, these angles change dramatically, with C_aNNC_a growing in size and C_bC_aNN shrinking. These geometrical changes tend to close the HOMO–LUMO gap, and one observes a series

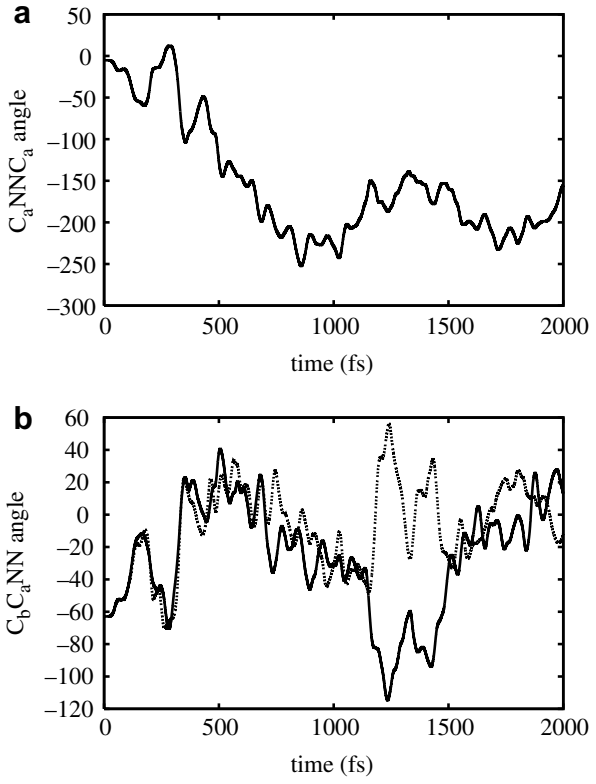

Fig. 3. Changes in (a) the C_aNNC_a dihedral angle and (b) the two C_bC_aNN dihedral angles resulting from application of a 100 fs (FWHM) laser pulse with a fluence of 0.473 kJ/m^2 and photon energy of 3.55 eV.

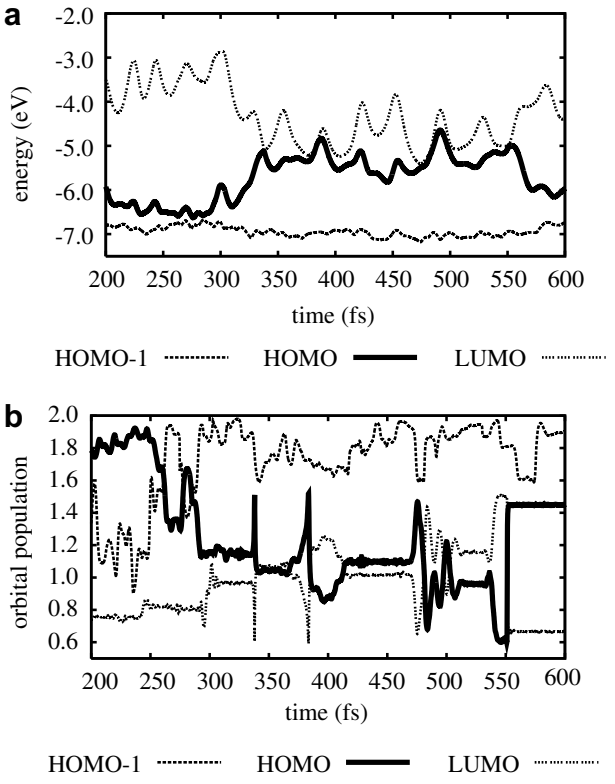

Fig. 4. Time evolution of molecular orbital (a) energy and (b) population following application of a 100 fs (FWHM) laser pulse with a fluence of 0.473 kJ/m^2 and photon energy of 3.55 eV.

of HOMO/LUMO avoided crossings between about 335 and 560 fs (See Fig. 4). During this time interval, the magnitude of the C_aNNC_a dihedral angle increases from 78° to 112°, while also exhibiting small amplitude oscillations.

The net result of this series of crossings is a transfer of 0.3 electrons back into the ground state. There are no subsequent population transfers between ground and excited states for the remainder of the simulation. The magnitude of the C_aNNC_a angle slowly grows until it reaches the fully *trans* value of 180° at 670 fs, while the two C_bC_aNN dihedral angles oscillate about nearly planar values for the remainder of the simulation. During the entire simulation, both of the central C_aNN bond angles oscillate between 100° and 130°, but never approach a linear configuration, demonstrating that inversion does not occur. The *cis* to *trans* reaction pathway for this simulation is clearly a rotation about the central NN bond.

In order to compare the present results to potential energy surface calculations, we interpret excitation out of the HOMO and into the LUMO as a transition to S_1, excitation out of the HOMO − 1 and into the LUMO as a transition to S_2, transfer of holes from HOMO − 1 to HOMO as $S_2 \rightarrow S_1$, and transfer of electrons from LUMO to HOMO as $S_1 \rightarrow S_0$. It should be emphasized that the above assignment is done strictly for comparative purposes, and that the work described here is complementary to previous theoretical treatments employing high-level multiconfigurational techniques. Although the present method is less accurate, it provides a more realistic picture of the processes during a photochemical reaction like photoisomerization, because it includes a superposition of molecular electronic states, rather than evolution along individual potential energy surfaces punctuated by transitions between these surfaces.

Note that the sequence of events observed in these simulations demonstrates that the full photoisomerization process involves both *multiple excited states* and *multiple steps*: Because of the complex interplay of nuclear and electron dynamics (and more fundamentally just because it is a quantum system), the molecule exists in a superposition of excited states at all times. In addition, the initial excitation proceeds in two stages, with the photon energy matched first to S_1, when the molecule starts in the ground-state geometry, and then to S_2, after nuclear motion results in a shift of the electronic energy levels. Finally, a sequence of avoided crossings is required to bring the molecule back into the new electronic ground-state for the *trans* configuration.

The need for multiple avoided crossings suggests a possible interpretation of the fact that the quantum yield for S_1 is significantly larger than that for S_2 [11]: In the case of S_1, isomerization can be achieved with a single transfer of electronic population, from S_1 to S_0, via a single avoided crossing. On the other hand, two steps are required in the case of S_2, involving both S_2/S_1 and S_1/S_0 avoided crossings. In a molecular orbital picture, first holes have to be transferred from HOMO − 1 to HOMO, and only then can the HOMO accept electrons from the LUMO in the second avoided crossing.

Acknowledgements

This work was supported by the Robert A. Welch Foundation (Grant A-0929). P.S. also thanks the Texas A&M Supercomputer Facility for the use of its parallel computing resources.

References

[1] See e.g.: J. Li, G. Speyer, O.F. Sankey, Phys. Rev. Lett. 93 (2004) 248302.
[2] D. Dulić et al., Phys. Rev. Lett. 91 (2003) 207402.
[3] C. Zhang, M.-H. Du, H.-P. Cheng, X.-G. Zhang, A.E. Roitberg, J.L. Krause, Phys. Rev. Lett. 92 (2004) 158301.
[4] Z.F. Liu, K. Hashimoto, A. Fujishima, Nature 347 (1990) 658.
[5] (a) T. Ikeda, T. Sasaki, K. Ichimura, Nature 361 (1993) 428;
(b) T. Ikeda, O. Tsutsumi, Science 268 (1995) 1873.
[6] T. Hugel, N.B. Holland, A. Cattani, L. Moroder, M. Seitz, H.E. Gaub, Science 296 (2002) 1103.
[7] R.H. Berg, S. Hvilsted, P.S. Ramanujam, Nature 383 (1996) 505.
[8] K. Ichimura, S.-K. Oh, M. Nakagawa, Science 288 (2000) 1624.
[9] S. Spörlein et al., Proc. Natl. Acad. Sci. USA 99 (2002) 7998.
[10] M. Volgraf, P. Gorostiza, R. Numano, R.H. Kramer, E.Y. Isacoff, D. Trauner, Nature Chem. Bio. 2 (2006) 47.
[11] P. Bortolus, S. Monti, J. Phys. Chem. 83 (1979) 648.
[12] T. Nägele, R. Hoche, W. Zinth, J. Wachtveitl, Chem. Phys. Lett. 272 (1997) 489.
[13] S. Monti, G. Orlandi, P. Palmieri, Chem. Phys. 71 (1982) 87.
[14] T. Ishikawa, T. Noro, T. Shoda, J. Chem. Phys. 115 (2001) 7503.
[15] A. Cembran, F. Bernardi, M. Garavelli, L. Gagliardi, G. Orlandi, J. Am. Chem. Soc. 126 (2004) 3234.
[16] E. Diau, J. Phys. Chem. A 108 (2004) 950.
[17] M. Tiago, S. Ismail-Beigi, S.G. Louie, J. Chem. Phys. 122 (2005) 094311.
[18] (a) C. Ciminelli, G. Granucci, M. Persico, Chem. Eur. J. 10 (2004) 2327;
(b) A. Toniolo, C. Ciminelli, M. Persico, T.J. Martinez, J. Chem. Phys. 123 (2005) 234308.
[19] P. Cattaneo, M. Persico, Phys. Chem. Chem. Phys. 1 (1999) 47739.
[20] L. Gagliardi, G. Orlandi, F. Bernardi, A. Cembran, M. Garavelli, Theor. Chem. Acc. 111 (2004) 363.
[21] Y. Dou, B.R. Torralva, R.E. Allen, J. Mod. Opt. 50 (2003) 2615.
[22] A.H. Zewail, Pure Appl. Chem. 72 (2000) 2219.
[23] P. Sauer, Y. Rostovtsev, R.E. Allen, J. Chem. Phys. 126 (2007) 024502.
[24] D. Porezag, Th. Frauenheim, Th. Köhler, G. Seifert, R. Kaschner, Phys. Rev. B 51 (1995) 947.
[25] P. Sauer, R.E. Allen, J. Mod. Opt. 53 (2006) 2619.
[26] H. Fliegl, A. Köhn, C. Hättig, R. Ahlrichs, J. Am. Chem. Soc. 125 (2003) 9821.
[27] G. Füchsel, T. Klamroth, J. Dokić, P. Saalfrank, J. Phys. Chem. B 110 (2006) 16337.